·临床研究·

结构性MRI测量对脊髓小脑共济失调3型的诊断价值

曾文婷[1]，赵　静[1]，胡曼诗[1]，丘海珊[1]，吴　超[2]，初建平[1]
(1. 中山大学附属第一医院放射科，广东 广州 510080；2. 中山大学附属第一医院神经科，广东 广州 510080)

摘　要：【目的】本研究拟探讨结构性MRI测量对脊髓小脑共济失调3型(SCA3)的诊断价值，并进一步评估其与疾病的严重程度及病程的相关性。【方法】前瞻性收集2018年5月至2021年11月于中山大学附属第一医院经基因诊断确诊的SCA3患者81例(症状组(sym-SCA3)：59，症状前组(pre-SCA3)：22，同时收集年龄、性别匹配的正常对照(HCs)35例。受试者均采集MRI结构像(3D T1WI MPRAGE)并收集其相应的临床资料。三位具不同临床经验的观察者分别通过第三方软件测量双侧小脑上、中、下脚宽度、脑桥及不同平面脊髓前后径(平枕骨大孔、颈$_{3-5}$椎体上缘)，其中一位观察者2个月后对上述指标进行重复测量。分别计算观察者内及观察者间可重复性，采用单因素方差分析、秩和检验、ROC曲线及随机森林方法评估上述指标对SCA3的诊断价值，并与临床资料进行相关性分析。【结果】基于形态学MRI脑结构测量指标，无论是观察者内或观察者间，均具有较高的可重复性且不依赖于观察者的临床经验，其中双侧小脑上、中脚具有最高的一致性。HCs、pre-SCA3和sym-SCA3三组的双侧小脑上、中、下脚、脑桥及脊髓前后径(除颈5椎体上缘水平)分别依次减小并具有统计学差异(P<0.017)。ROC示左侧小脑中脚对pre-SCA3的诊断价值最高(AUC=0.911)，其敏感度、特异度和cut-off值分别为85.7%，95.5%和10.15 mm，而右侧小脑上脚对sym-SCA3的诊断价值最高(AUC=0.999)，其临界值为2.62 mm，敏感度和特异度分别是100%和98.3%。进一步，基于上述指标的随机森林模型区分三组同样有着很高的诊断效能(AUC=0.970，特异度=93.1%)，其中左侧小脑中脚对模型的贡献度最大。此外，相关分析表明上述指标同SARA和病程存在中等程度或显著负相关(P<0.05)。【结论】基于形态学MRI的脑结构测量可重复性好、不依赖于临床经验，可以帮助诊断SCA3并预测疾病的严重程度和病程，左侧小脑中脚及右侧小脑上脚分别用于预测pre-SCA3和sym-SCA3价值最优。由此，本研究推荐临床纳入MRI脑结构测量协助评估SCA3。

关键词：脊髓小脑共济失调3型；MRI；脑结构测量；诊断
中图分类号：R739.41　　**文献标志码**：A　　**文章编号**：1672-3554(2023)01-0106-09
DOI：10.13471/j.cnki.j.sun.yat-sen.univ(med.sci).2023.0114

Diagnostic Value of Structural MRI in Spinocerebellar Ataxia Type 3

ZENG Wen-ting[1], ZHAO Jing[1], HU Man-shi[1], QIU Hai-shan[1], WU Chao[2], CHU Jian-ping[1]
(1. Department of Radiology, The First Affiliated Hospital of Sun Yat-sen University, Guangzhou 510080, China;
2. Department of Neurology, The First Affiliated Hospital of Sun Yat-sen University, Guangzhou 510080, China)
Correspondence to: CHU Jian-ping; E-mail: chujping@mail.sysu.edu.cn

Abstract: 【Objective】To explore the role of structural MRI in the diagnosis of spinocerebellar ataxia type 3 (SCA3) and further evaluate its correlation with disease severity and disease duration. 【Methods】We prospectively enrolled 81 genetically diagnosed SCA3 patients [59 symptomatic (sym-SCA3) and 22 pre-symptomatic (pre-SCA3)] and 35 age- and sex-matched healthy controls (HCs). MRI structural images (3D T1 MPRAGE) and clinical data of all subjects were collected. Three observers with different radiological experience measured the width of the superior, middle and inferior cere-

收稿日期：2022-09-01
基金项目：国家自然科学基金(82172015)；广东省基础与应用基础研究基金(2022A1515011264，2021A1515012279)
作者简介：曾文婷，硕士生，研究方向：神经系统影像诊断，E-mail：zengwt23@mail2.sysu.edu.cn；；初建平，通信作者，硕士生导师，主任医师，E-mail：chujping@mail.sysu.edu.cn

bellar peduncle (SCP, MCP and ICP), the anterior-posterior diameters of the pons and spinal cord at the levels of the foramen magnum and upper edge of the 3rd-5th cervical vertebra. One observer performed the measurements again 2 months later to assess for the intra- and inter-observer reliability, respectively. One-way ANOVA, rank-sum test, ROC curve and Random Forest were used to evaluate the diagnostic value of the above metrics for SCA3, and the correlation between the metrics and clinical variables was analyzed.【Results】Not depending on the radiological experience, the metrics based on morphological MRI showed high intra- and inter-observer reliability, among which bilateral superior and middle cerebellar peduncles performed best. The diameters of bilateral SCP, MCP, ICP, pons and spinal cord (except spinal cord at the level of the upper edge of the 5th cervical vertebra) decreased successively in HCs, pre-SCA3 and sym-SCA3 with a statistical difference (P<0.017). ROC analysis revealed that the left MCP had the highest diagnostic value for pre-SCA3 (AUC=0.911), with sensitivity, specificity and a cut-off value of 85.7%, 95.5% and 10.15 mm, respectively. In contrast, the right SCP had the highest diagnostic value for sym-SCA3 (AUC=0.999), with sensitivity, specificity and a cut-off value of 100%, 98.3% and 2.62 mm, respectively. The Random Forest model based on the above metrics also had high diagnostic efficiency (AUC= 0.970, specificity=93.1%), and the left MCP contributed the most. Correlation analysis showed that the above metrics had a significantly or moderately negative correlation with the Scale for the Assessment and Rating of Ataxia (SARA) and disease duration (P<0.05).【Conclusion】Not depending on radiological experience, measurements of brain structure based on morphological MRI are reliable, which can help diagnose SCA3 and predict disease severity and duration. The left MCP and the right SCP perform best for predicting pre-SCA3 and sym-SCA3, respectively. Therefore, the structural MRI is recommended for assisting the clinical diagnosis of SCA3.

Key words: spinocerebellar ataxia type 3 (SCA3); MRI; brain structural measurement; diagnosis

[J SUN Yat-sen Univ(Med Sci),2023,44(1):106-114]

脊髓小脑共济失调(spinocerebellar ataxias,SCAs)是一组临床和遗传异质性的常染色体显性遗传神经变性病,包括40多个不同的亚型[1]。SCA3是最常见的亚型,约占20%~50%[2]。进行性小脑共济失调是SCA3的特征性表现,主要通过SARA量表[3]进行评估。目前SCA3主要依赖基因诊断,但基因检测费用相对昂贵,尤其是应用于筛查SCA3潜在患病者。目前临床上只对明确存在SCA3证据指向的病人进行基因检查,这也潜在增加了SCA3的漏诊率,尤其对于症状前SCA3。因此,亟需开发新的无创检查协助临床筛选患者进行基因检测。目前MRI广泛应用于SCA3的诊断及随访评估。研究表明,SCA3的疾病发生及进展是由幕下逐渐至幕上的过程;与正常对照相比,症状组SCA3患者的中枢神经系统广泛受累,主要表现广泛的白质、小脑及基底节受累,而皮层受累相对较轻[4]。症状前SCA3(pre-symptomatic SCA3,pre-SCA3)患者在出现共济失调症状之前也已出现脑干、黑质和脊髓的体积减小及小脑脚各向异性分数(fractional anisotropy, FA)的减低[5-8]。然而,上述研究需通过繁杂的后处理分析,临床推广价值有限。而不需要借助后处理分析软件的幕下MRI结构测量将大大提高临床应用的可行性[9],这已经应用于SCA及其他神经退行性疾病[10-11]。Higashi[10]等研究发现,与其他引起小脑共济失调的疾病相比,SCAs的脑桥基底与被盖的距离比(the distance ratio of pontine base to tegmentum,BT ratio)更高。同时Reetz等[12]研究表明,与正常人相比,SCA2患者的脑桥前后径明显缩小。由此,本研究纳入症状组SCA3(symptomatic SCA3,sym-SCA3)、pre-SCA3及健康对照,测量双侧小脑脚宽度、脑桥前后径及脊髓前后径,评估上述MRI测量指标对SCA3的诊断价值并进一步评估上述指标与SARA和病程的相关性。

1　材料与方法

1.1　一般资料

本研究已获得中山大学附属第一医院研究伦理委员会批准,患者已签署知情同意书。前瞻性收集2018年5月至2021年11月经基因诊断确诊的SCA3成年患者81例,进行颅脑磁共振扫描。排除标准如下:① 合并其他精神障碍或精神药物依赖;② MRI图像质量存在伪影,无法进行图像分析;③合并其他大脑器质性病变和/或代谢性疾病史;④ 孕妇和哺乳期妇女;⑤ 其他MRI扫描禁忌症。同时,招募35名无共济失调和/或遗传性神经变性病家族史的健康对照(healthy controls, HCs)。

所有SCA3患者均接受详细的神经系统检查,并使用SARA量表评估疾病的严重程度[13]。SCA3患者分为症状组(sym-SCA3,SARA评分≥3)和症状前组(pre-SCA3,SARA评分<3)[14]。

1.2　MRI检查方法

采用德国Siemens Magnetom Verio 3.0T MRI扫描仪及20通道头颅相控阵线圈进行数据采集。扫描的序列包括矢状位3D T_1WI MPRAGE、轴位T_2WI、轴位T2液体衰减反转

恢复序列(T2-fluid attenuated inversion recovery, T2-FLAIR)。3D T_1WI MPRAGE扫描参数:TR 1 750 ms,TE 2.8 ms,层厚 0.7 mm,层间距 0 mm,FOV 260 mm×260 mm,256层;T_2WI 参数:TR 4 000 ms,TE 100 ms,层厚 5.0 mm,层间距 0.5 mm,FOV 230 mm×230 mm,19层;FLAIR 参数:TR 9 000 ms,TE 81 ms,反转时间(inversion time,TI)2 500 ms,层厚 6.0 mm,层间距 1.2 mm,FOV 230 mm×230 mm,19层。

1.3 MRI的结构测量指标及观察者一致性分析

在矢状位3D T_1WI MPRAGE图像上测量双侧小脑中脚(middle cerebellar peduncle,MCP)、小脑上脚(superior cerebellar peduncle,SCP)、小脑下脚(inferior cerebellar peduncle,ICP)和平枕骨大孔及C_{3-5}上缘水平的脊髓前后径(anterior-posterior diameters of spinal cord at levels of the foramen magnum and upper edge of the 3rd-5th cervical vertebra,SC_{0-3})[11]。在轴位T_2WI测量脑桥基底部前后径(anterior-posterior diameter of pontine base,a)和脑桥被盖前后径(anterior-posterior diameter of pontine tegmentum,b)(表1,图1),并计算BT ratio,即a与b的比率[10]。此外,本研究还纳入计算脊髓前后径变异率(Variation)和脊髓前后径减小量(L_{reduce})。其中对于每个患者,Variation $=\sqrt{(SC_0-Mean)^2}+\sqrt{(SC_1-Mean)^2}+\sqrt{(SC_2-Mean)^2}+\sqrt{(SC_3-Mean)^2}$(Mean是$SC_0$到$SC_3$的平均值)及$L_{reduce}=SC_0-SC_3$。

在未知患者诊断的情况下,一位具有3年放射诊断经验的医生(观察者1)对所有MRI图像的上述参数进行测量。为评估观察者内部及观察者间一致性,在第一次测量两个月后观察者1对所有图像进行第二次测量(图像的顺序随机排列)。另外两名观察者随机选择60例受试者的图像对上述参数进行测量,以评估不同观察者之间的测量可重复性。在这两名观察者中,一名是具有20年放射诊断经验的神经放射学医生(观察者2),另一名是几乎没有放射学经验的医学本科生(观察者3)。所有参数均在Radiant软件(2021.2.2.35002版本)上测量。

表1 相关结构的MRI测量标准

Table 1 Morphological MRI Measurement details of included metrics

Metrics	Sequence	Section	Level	Linear measurement
MCP	3D-T1 MPRAGE	Sagittal	Parasagittal view that best exposed the MCP between the pons and the cerebellum	The linear distance between the superior and inferior borders of the MCP, as delimited by the peripeduncular cerebrospinal fluid spaces of the pontocerebellar cisterns
ICP	3D-T1 MPRAGE	Sagittal	Level that best exposed the ICP	The maximum distance between the two points where the ICP intersects its vertical line
SCP	3D-T1 MPRAGE	Sagittal	Level of separation of SCP and inferior colliculus	The maximum distance between the two points where the SCP intersects its vertical line
SC_{0-3}	3D-T1 MPRAGE	Sagittal	Levels that best exposed SC (SC_{0-3})	The maximum distance at the levels of the foramen magnum and upper edge of the 3rd-5th cervical vertebra between the two points where the SC intersects its vertical line
a	T_2WI	Axial	Level where the MCP were observed largest	The distance from the ventral edge of the pons to the ventral border of the medial lemniscus
b	T_2WI	Axial	Level where the MCP were observed largest	The distance from the ventral edge of the medial lemniscus to the dorsal edge of the pons

MCP: middle cerebellar peduncle, ICP: inferior cerebellar peduncle, SCP: superior cerebellar peduncle, SC_{0-3}: the anterior-posterior diameters of spinal cord at levels of the foramen magnum and upper edge of the 3rd-5th cervical vertebra, SC: spinal cord, a: anterior-posterior diameter of pontine base , b: anterior-posterior diameter of pontine tegmentum.

1.4 统计学方法

采用IBM SPSS Statistics 25软件对数据进行统计学分析。利用Shapiro-Wilk和Levene检验对各定量参数进行正态性检验和方差齐性检验。连续变量用均数±标准差表示。使用组内相关系数(interclass correlation coefficient,ICC)评估观察者内部及观察者间的测量一致性。使用卡方检验比较三组的性别差异。若连续变量呈正态性分布、方差齐,采用方差分析;若非正态分布或方差不齐,则采用非参数检验的Kruskal-Wallis H检验比较各组的形态学测量参数,差异有统计学意义时采用Bonferroni法进行组间两两比较,组间两两比较以$P<0.017$为差异有统计学意义。利用特征性曲线(receiver operating characteristic curve,ROC curve)分析各形态学测量参数诊断SCA3(区分sym-SCA3及HCs、pre-SCA3及HCs)的效能。

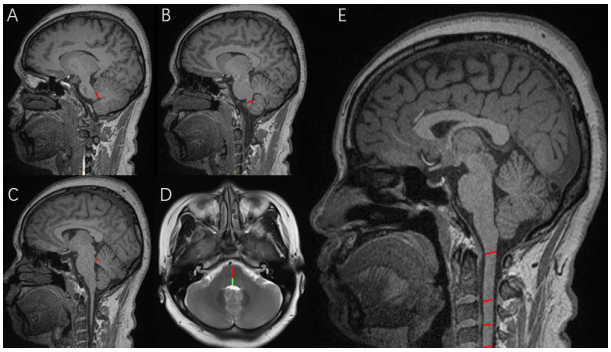

A-C: Measurement of middle cerebellar peduncle, inferior cerebellar peduncle, and superior cerebellar peduncle. D: Measurements of the anterior-posterior diameter of pontine base ("a") and pontine tegmentum ("b") on T2 weighted axial magnetic resonance imaging (MRI) scan. The medial lemniscus was identified as boundary lines between lower intensity and higher intensity. The distance of the pontine base was measured as the distance from the ventral edge of the pons to the medial lemniscus, marked as "a" (red line). The length of the pontine tegmentum was measured as the distance from the medial lemniscus to the dorsal edge of the pons, marked as "b"(green line). E: The anterior-posterior diameters of the spinal cord at levels of the foramen magnum and upper edge of the 3rd-5th cervical vertebra (SC_{0-3}). The maximum diameters of SC_0- SC_3 may not be shown on the same slice.

图1　基于形态学MRI的脑结构测量指标示例图

Fig. 1　An example of morphological measurement of included metrics

在Python软件(3.10.0版本)采用十折交叉验证划分训练集和测试集。基于训练集，以形态学MRI测量参数作为解释变量，受试者组别(sym-SCA3、pre-SCA3、HCs)为结局变量，构建随机森林。随机森林模型的参数设置为最大树深3，固定树数100。在测试集中，评价决策树的敏感度、特异度和ROC曲线下面积(AUC)。重复上述步骤1 000次，得到各统计量的抽样分布。

基于形态学的脑结构测量参数与临床评分之间的相关性分析采用Pearson(正态分布数据)或Spearman相关分析法(非正态分布数据)。结果均选择双侧假设检验，以P<0.05为差异有统计学意义。

2　结 果

2.1　一般临床资料

本研究纳入的sym-SCA3组与HCs组的年龄(t=5.430，P=0.449)与性别(χ^2=0.115，P=0.734)差异均无统计学意义，而pre-SCA3组与其余两组的年龄与性别差异具有统计学意义(表2)。

2.2　观察者内部和观察者之间的一致性检验

大多数参数的观察者内部和观察者之间的测量一致性为"一致性较好"或"一致性极好"(表3)。在所有参数中，双侧MCP、SCP、SC_1的ICC最高。

2.3　基于形态学MRI的脑结构测量对pre-SCA3和sym-SCA3的诊断价值

① pre-SCA3 vs HCs　同HCs相比，pre-SCA3的双侧MCP、SCP及ICP、SC_{0-2}、b和Variation明显减低(图2)。

ROC分析示左侧小脑中脚(left middle cerebellar peduncle，LMCP)预测pre-SCA3有着最佳的诊断价值AUC(95%CI)=0.911(0.830，0.992)，P<0.001，其敏感度、特异度和cut-off值分别为85.7%，95.5%和10.15 mm；此外，右侧小脑中脚(right middle cerebellar peduncle，RMCP)(cut-off：9.8 mm)和右侧小脑上脚(right superior cerebellar peduncle，RSCP)(cut-off：2.9 mm)在预测pre-SCA3分别展现出最高的敏感度(97.0%)，而LMCP(cut-off：10.15 mm)展现出最高的特异度(95.5%；图3A)。

② sym-SCA3 vs HCs　同HCs相比，sym-SCA3的双侧MCP、SCP及ICP、SC_{0-3}、脑桥基底部前后径(a)、脑桥被盖部前后径(b)、脊髓前后径变异率(Variation)明显减低。同HCs相比，sym-SCA3的BT ratio增大(图2)。

ROC分析示RSCP预测sym-SCA3有着最佳的诊断价值AUC(95%CI)=0.999(0.996，1.00)，P< 0.001，及最佳的敏感度(100%)和特异度(98.3%)，其cut-off值为2.62 mm(图3B)。

sym-SCA3 vs pre-SCA3　同pre-SCA3相比，sym-SCA3的双侧MCP、SCP及ICP、SC_{0-3}、a、b明显减低(图2)。

表2　纳入受试者的主要临床信息

Table 2　The clinical information of included subjects　($\bar{x}\pm s$)

Items	sym-SCA3 (n=59)	pre-SCA3 (n=22)	HCs (n=35)	$H/\chi^2/t$	P
Age/years	39.9±10.8	29.0±8.2	38.6±12.1	16.790	<0.001
Gender/(M/F)	24/35	16/6	13/22	8.109	0.017
Disease duration/years	5.50±3.60	0.14±0.35	/	6.878	<0.001
SARA	12.80±6.40	0.50±0.67	/	8.905	<0.001

Continuous variables are expressed as ($\bar{x}\pm s$). Disease duration was computed as the difference between age at scan and reported age at onset. SARA: the scale for the assessment and rating of ataxia.

表3 观察者内部和观察者之间的组内相关系数

Table 3 Interclass correlation coefficient values of included morphological metrics among different observers

Metrics	ICC1	ICC2	ICC3
RMCP	0.83	0.79	0.68
RICP	0.76	0.57	0.84
RSCP	0.76	0.74	0.79
LSCP	0.83	0.68	0.71
LICP	0.66	0.43	0.78
LMCP	0.80	0.72	0.73
SC_0	0.90	0.52	0.73
SC_1	0.86	0.77	0.76
SC_2	0.70	0.65	0.72
SC_3	0.71	0.75	0.76
a	0.73	0.78	0.46
b	0.63	0.75	0.71

ICC1: intra-observer agreement of evaluator 1, ICC2: ICC between observer 1 and 2, ICC3: ICC between observer 1 and 3. RMCP: right middle cerebellar peduncle, RICP: right inferior cerebellar peduncle, RSCP: right superior cerebellar peduncle, LMCP: left middle cerebellar peduncle, LICP: left inferior cerebellar peduncle, LSCP: left superior cerebellar peduncle, SC_{0-3}: anterior-posterior diameters of the spinal cord at levels of the foramen magnum and the upper edge of the 3rd-5th cervical vertebra, "a": anterior-posterior diameter of pontine base, "b": anterior-posterior diameter of pontine tegmentum.

ROC分析示LMCP鉴别sym-SCA3与pre-SCA3有着最佳的诊断价值AUC(95%CI)= 0.923(0.866, 0.979), P<0.001,其敏感度、特异度和cut-off值分别为90.9%,86.4%和8.58 mm;此外,RMCP(cut-off:8.35 mm)鉴别sym-SCA3与pre-SCA3展现出最高的敏感度(100%;图3C)。

2.4 随机森林用于SCA3的诊断价值

基于随机森林,利用MRI形态学测量参数构建区分HCs、sym-SCA3和pre-SCA3的预测模型并绘制ROC曲线(图4),结果显示基于MRI形态学测量的随机森林模型具有很高的预测价值AUC(95%CI)=0.970(0.961, 0.973), P < 0.001,其敏感度和特异度分别为86.2%和93.1%。其中,对区分三者的最重要的五个形态学测量参数分别是LMCP,RSCP,左侧小脑上脚(left superior cerebellar peduncle,LSCP),RMCP和左侧小脑下脚(left inferior cerebellar peduncle,LICP),LMCP是最重要的测量参数。

2.5 基于MRI形态学的测量参数与临床特征的相关性

不管是pre-SCA3或者sym-SCA3患者,除BT ratio和L_{reduce}外,上述形态学测量参数均与病程和SARA之间存在显著或中等程度负相关,其中Variation表现出与病程(r= −0.70, P<0.001)和SARA(r= −0.68, P<0.001)最强的负相关。

亚组分析显示,对于sym-SCA3,LSCP、SC_2、SC_3、a及Variation与病程呈中度负相关,SC_{1-3}、a及Variation与SARA呈中等程度负相关,a表现出与病程(r= −0.55, P<0.001)最强的负相关,且a与SARA有最强的负相关(r = −0.55, P< 0.001)。对于pre-SCA3,RSCP、LSCP、SC_{1-3}和Variation与SARA存在显著或中等程度负相关,而Variation同SARA表现出最强的负相关(r = −0.64, P<0.001;表5)。

3 讨 论

本文研究结果表明,基于MRI的形态学测量可以用于区分pre-SCA3和sym-SCA3,其中左侧小脑中脚及右侧小脑上脚分别有着最佳诊断效能。此外,基于MRI的形态学测量参数建立的随机森林模型对sym-SCA3、pre-SCA3、HCs三组有着更高的分类诊断效能,ROC曲线下面积达0.970,敏感度86.2%,特异度93.1%。进一步的相关分析表明上述基于MRI的形态学测量参数与SCA3患者的病程和SARA显著相关。

尽我们所知,我们的研究首次探讨了双侧小脑脚、脑桥和脊髓宽度(平枕骨大孔及C_{3-5}上缘水平)对SCA3的诊断价值。大多数形态学参数的观察者内部及观察者之间一致性为"一致性较好"或"一致性极好",这表明具有不同经验的同行的测量可重复性好,本研究中使用的形态学测量方法简单、可靠且可行。部分形态学参数的ICC较低可能是由于本研究中一位观察者是医学本科生,没有影像诊断的实际经验,培训时间较短。然而,纳入具备相关解剖基础的本科生,可以进一步有效地评价该测量方法的可重复性和稳定性,为研究结果推向临床奠定基础。

sym-SCA3、pre-SCA3和HCs三组间测量值的比较显示,大多数MRI形态学参数的两两比较均具有统计学差异,尤其是双侧小脑脚,这与前人的研究基本一致[7, 15-17]。Rezende[6]等利用脑结构MRI及扩散张量成像发现,pre-SCA3存在右侧小脑上、中、下脚的白质损伤和脑干及脊髓的萎缩,而sym-SCA3存在广泛的白质纤维损伤及脑实质萎缩。另外,Peng[16]等及Fahl[17]等的研究同样发现,与正常对照相比,sym-SCA3的小脑上、中、下脚FA值减低,脑桥及脊髓面积缩小。上述研究使用的高级扩散加权序列及基于多种模型的复杂分割技术,虽可敏感及早期检出SCA3异常,但处理过程复杂且耗时,临床推广价值有限。而本研究结果表明,基于结构性MRI测量,已能识别上述研究所提及的pre-SCA3及sym-SCA3与正常对照的差异,这种方法简单、省时并具备一定的临床推广价值。虽然我们缺乏纵向研究数据,但HCs、pre-SCA3、sym-SCA3三组可看作SCA3患者病情从轻到重的不同阶段,三组的双侧MCP、ICP、SCP、SC_0、SC_1、SC_2的测量值分别逐次减小并具有统计学意义,这与

表4　sym-SCA3，pre-SCA3和HCs的参数比较

Table 4　The comparison of metrics among sym-SCA3，pre-SCA3 and HCs

Metrics/mm	sym-SCA3	pre-SCA3	HCs	*F/H*	*P*	t/Z HCs vs pre-SCA3/ HCs vs sym-SCA3/ pre-SCA3 vs sym-SCA3	P pre-SCA3 vs HCs/sym-SCA3 vs HCs/ sym-SCA3 vs pre-SCA3
RMCP	7.33±0.18	9.45±0.17	10.91±0.14	79.897	<0.001	27.516/63.188/35.671	0.003[1)]/<0.001[1)]/<0.001[1)]
RICP	6.20±0.10	7.03±0.15	7.86±0.10	62.552	<0.001	4.635/11.177/4.540	<0.001[1)]/<0.001[1)]/0.001[1)]
RSCP	1.67±0.10	2.31±0.15	3.41±0.10	75.932	<0.001	34.379/62.370/27.991	<0.001[1)]/<0.001[1)]/0.001[1)]
LSCP	1.82±0.11	2.45±0.14	3.42±0.10	70.209	<0.001	32.663/59.948/27.285	<0.001[1)]/<0.001[1)]/0.001[1)]
LICP	6.31±0.10	7.15±0.15	7.85±0.11	61.596	<0.001	22.806/55.282/32.475	0.013[1)]/<0.001[1)]/<0.001[1)]
LMCP	7.19±0.19	9.39±0.14	10.77±0.14	83.372	<0.001	27.440/64.452/37.012	0.003[1)]/<0.001[1)]/<0.001[1)]
SC_0	7.63±0.13	8.39±0.15	9.34±0.15	48.992	<0.001	27.137/50.072/22.935	0.003[1)]/<0.001[1)]/0.006[1)]
SC_1	6.61±0.11	7.21±0.10	7.98±0.13	49.245	<0.001	28.412/50.271/21.859	0.002[1)]/<0.001[1)]/0.009[1)]
SC_2	6.11±0.11	6.70±0.11	7.22±0.11	26.471	<0.001	3.283/6.810/3.106	0.002[1)]/<0.001[1)]/0.003[1)]
SC_3	5.52±0.12	6.32±0.14	6.71±0.10	41.753	<0.001	14.753/44.775/30.022	0.107/<0.001[1)]/<0.001[1)]
a	13.16±0.23	15.13±0.36	14.87±0.23	17.979	<0.001	−0.639/4.939/4.546	0.525/<0.001[1)]/<0.001[1)]
b	4.75±0.10	5.84±0.12	6.36±0.14	54.599	<0.001	2.534/9.622/6.190	0.014[1)]/<0.001[1)]/<0.001[1)]
BT ratio	2.84±0.11	2.63±0.10	2.38±0.10	8.679	<0.001	−2.165/−4.059/−1.516	0.035/<0.001[1)]/0.134
Variation	2.88±0.13	2.53±0.18	3.55±0.20	7.691	0.001	3.577/2.937/−1.459	0.001[1)]/0.004[1)]/0.149
L_{reduce}	0.27±0.01	0.24±0.02	0.28±0.01	1.130	0.327	1.615/0.205/−1.273	0.112/0.838/0.207

RMCP：right middle cerebellar peduncle，RICP：right inferior cerebellar peduncle，RSCP：right superior cerebellar peduncle，LSCP：left superior cerebellar peduncle，LICP：left inferior cerebellar peduncle，LMCP：left middle cerebellar peduncle，SC_{0-3}：anterior-posterior diameters of spinal cord at levels of the foramen magnum and upper edge of the 3rd-5th cervical vertebra，“a”：anterior-posterior diameter of pontine base，“b”：anterior-posterior diameter of pontine tegmentum，L_{reduce}：SC_0-SC_3，BT ratio：“a”/“b”，Variation = $\sqrt{(SC_0-Mean)^2}+\sqrt{(SC_1-Mean)^2}+\sqrt{(SC_2-Mean)^2}+\sqrt{(SC_3-Mean)^2}$（*Mean* is the mean value of SC_0 to SC_3），HCs：Healthy Controls. Two-tail，[1)] Pairwise comparison among groups，the difference is significant（$P<\alpha'=\alpha/3=0.017$）.

Rezende等[6]研究结论相仿：SCA3小脑脚的FA值随病程进展而减低，脊髓面积随病程进展而减小。这一研究结果提示，上述参数或可动态监测SCA3患者的疾病严重程度的变化。进一步，基于形态学参数，我们对sym-SCA3、pre-SCA3、HCs三组建立随机森林模型。ROC曲线分析表明，AUC可达到0.970。在随机森林分类器的重要性排名中，同样发现双侧小脑脚的贡献度最大。这均提示在本研究的测量参数里，小脑脚在动态观察疾病变化、理解病程发展、协助诊断方面作用更显著。

在相关性分析中，大多数形态学参数与病程和SARA呈显著或中度负相关，且参数在症状出现前就已有异常，比临床评分更早期识别异常，这意味着形态学测量可能是监测SCA3疾病进展的一种可靠方法。对退行性病变的患者而言，几乎不可能在疾病早期取得尸检结果，本文所测量的参数的异常有助于揭示SCA3患者疾病过程中相关结构的病理生理变化，尤其是在疾病早期。与HCs比较，pre-SCA3患者小脑脚的异常说明，即使尚未出现临床症状，小脑的传入和传出系统在SCA3的早期病程中已经受损。当就诊者有SCA3家族史而又未表现出临床症状时，若上述参数有异常，则强烈提示该就诊者患病的可能性，需进一步进行基因检测，如确诊后可早期开始治疗。

本研究需进一步完善，仍存在两点不足。首先pre-SCA3和HCs的年龄和性别不匹配，由于pre-SCA3来自具有SCA3家族史的未发病人群，所以pre-SCA3较HCs年轻，这可能会导致比较分析中存在一些偏倚；其次，pre-SCA3样本量较少，这可能导致结果的不稳定性。然而，本次研究的结果与以往研究结论相仿，在后续进一步研究中，我们将持续招募pre-SCA3患者及健康对照，以期获得更稳健的研究结果。

基于形态学MRI的脑结构测量可重复性好、不依赖于临床经验，可以帮助诊断SCA3并与疾病的严重程度和病程相关，左侧小脑中脚及右侧小脑上脚分别用于预测pre-和sym-SCA3价值最优。由此，本研究推荐临床纳入形态学MRI的脑结构测量协助评估SCA3。

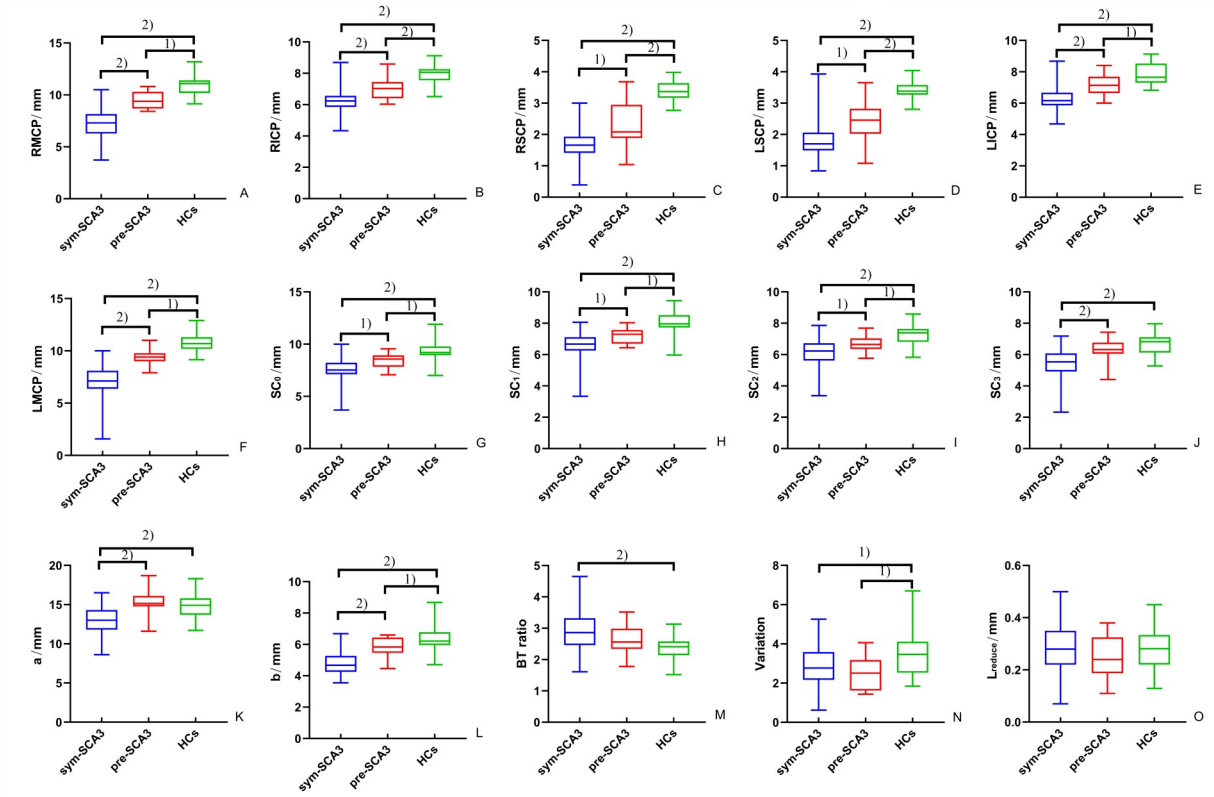

A–O: box plot of RMCP, RICP, RSCP, LSCP, LICP, LMCP, SC_{0-3}, a, b, BT ratio, Variation, L_{reduce} of included subjects. RMCP: right middle cerebellar peduncle, RICP: right inferior cerebellar peduncle, RSCP: right superior cerebellar peduncle, LSCP: left superior cerebellar peduncle, LICP: left inferior cerebellar peduncle, LMCP: left middle cerebellar peduncle, SC_{0-3}: the anterior–posterior diameters of spinal cord at the level of the foramen magnum and upper edge of the 3rd–5th cervical vertebra, "a": anterior–posterior diameter of pontine base , "b": anterior–posterior diameter of pontine tegmentum, BT ratio: "a"/"b", Variation = $\sqrt{(SC_0 - Mean)^2} + \sqrt{(SC_1 - Mean)^2} + \sqrt{(SC_2 - Mean)^2} + \sqrt{(SC_3 - Mean)^2}$ (*Mean* is the mean value of SC_0 to SC_3) , L_{reduce}: $SC_0 - SC_3$. 1) $P<0.017$, 2) $P<0.001$.

图2 三组间所有参数两两比较箱形图

Fig. 2 box plot of pairwise comparison of all metrics among three groups

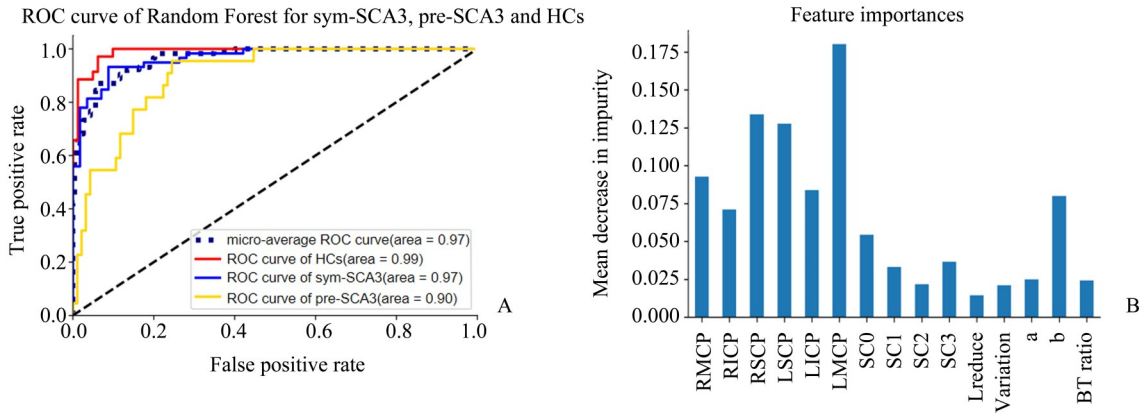

A: ROC curve of Random Forest for sym–SCA3, pre–SCA3 and HCs AUC (95%CI) =0.970 (0.961, 0.973), P <0.001. B: Bar chart of feature importances of metrics in Random Forest.

图4 基于随机森林模型,形态学参数鉴别HCs、sym–SCA3、pre–SCA3的ROC曲线及特征重要性图

Fig. 4 ROC curves and bar chart of feature importances of identification of HCs, sym–SCA3 and pre– SCA3 by metrics based on the Random Forest classifier

表5　总SCA3，sym-SCA3，pre-SCA3的参数和临床变量的相关系数

Table 5　Correlation coefficient of metrics and clinical variables of SCA3 taken together，sym-SCA3，pre-SCA3

Items	SCAs		sym-SCA3		pre-SCA3	
	Disease duration	SARA	Disease duration	SARA	Disease duration	SARA
RMCP	−0.64[2)]	−0.58[2)]	−0.33[1)]	/	/	/
RICP	−0.52[2)]	−0.43[2)]	−0.29[1)]	/	/	/
RSCP	−0.48[2)]	−0.42[2)]	/	/	/	−0.64[2)]
LSCP	−0.59[2)]	−0.48[2)]	−0.42[2)]	/	−0.49[1)]	−0.52[1)]
LICP	−0.57[2)]	−0.48[2)]	−0.36[2)]	/	/	/
LMCP	−0.67[2)]	−0.65[2)]	−0.34[2)]	−0.30[1)]	/	/
SC_0	−0.46[2)]	−0.52[2)]	−0.33[1)]	−0.37[2)]	/	−0.57[2)]
SC_1	−0.46[2)]	−0.53[2)]	−0.32[1)]	−0.44[2)]	/	−0.50[1)]
SC_2	−0.51[2)]	−0.54[2)]	−0.46[2)]	−0.50[2)]	/	−0.44[1)]
SC_3	−0.55[2)]	−0.56[2)]	−0.42[2)]	−0.44[2)]	0.44[1)]	−0.55[2)]
a	−0.60[2)]	−0.60[2)]	−0.55[2)]	−0.55[2)]	/	/
b	−0.54[2)]	−0.45[2)]	/	/	/	/
BT ratio	/	/	/	−0.35[2)]	/	/
Variation	−0.70[2)]	−0.68[2)]	−0.50[2)]	−0.43[2)]	−0.49[1)]	−0.64[2)]
L_{reduce}	0.34[2)]	0.29[1)]	0.27[1)]	/	/	/

RMCP：right middle cerebellar peduncle，RICP：right inferior cerebellar peduncle，RSCP：right superior cerebellar peduncle，LSCP：left superior cerebellar peduncle，LICP：left inferior cerebellar peduncle，LMCP：left middle cerebellar peduncle，SC_{0-3}：anterior-posterior diameters of spinal cord at levels of the foramen magnum and upper edge of the 3rd-5th cervical vertebra，“a”：anterior-posterior diameter of pontine base，“b”：anterior-posterior diameter of pontine tegmentum，L_{reduce}：SC_0 −SC_3，BT ratio：“a”/“b”，Variation = $\sqrt{(SC_0 - Mean)^2} + \sqrt{(SC_1 - Mean)^2} + \sqrt{(SC_2 - Mean)^2} + \sqrt{(SC_3 - Mean)^2}$（*Mean* is the mean value of SC_0 to SC_3），HCs：Healthy Controls. Two-tail，[1)] $P<0.05$，[2)] $P<0.001$.

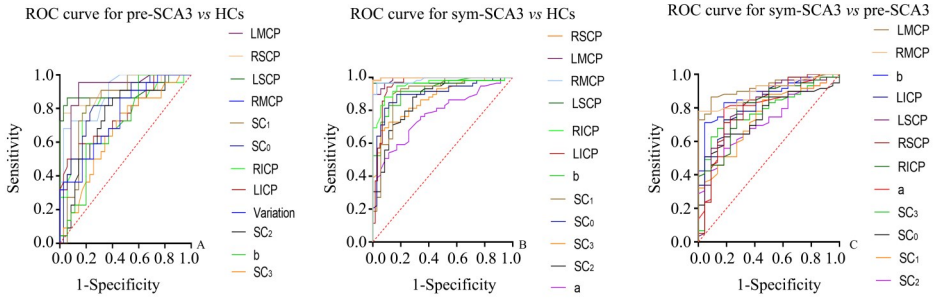

The labels on the right side of each figure was ranked by the value of ROC with $P<0.05$. A: ROC analysis showed that LMCP had the highest diagnostic value for pre-SCA3 AUC (95%CI) =0.911 (0.830, 0.992), $P<0.001$, with sensitivity, specificity, and cut-off value of 85.7%, 95.5% and 10.15 mm, respectively. B: ROC analysis showed that RSCP had the highest diagnostic value for sym-SCA3 AUC (95%CI) =0.999 (0.996, 1.00), $P<0.001$, with sensitivity, specificity and cut-off value of 100%, 98.3% and 2.62 mm, respectively. C: ROC analysis showed that LMCP had the highest value for differentiating sym-SCA3 and pre-SCA3 AUC (95%CI)=0.923 (0.866, 0.979), $P<0.001$, with sensitivity, specificity and cut-off value of 90.9%, 86.4% and 8.58 mm, respectively. RMCP: right middle cerebellar peduncle, RICP: right inferior cerebellar peduncle, RSCP: right superior cerebellar peduncle, LSCP: left superior cerebellar peduncle, LICP: left inferior cerebellar peduncle, LMCP: left middle cerebellar peduncle, SC_{0-3}: anterior-posterior diameters of spinal cord at levels of the foramen magnum and upper edge of the 3rd-5th cervical vertebra, “a”: anterior-posterior diameter of pontine base, “b”: anterior-posterior diameter of pontine tegmentum, Variation = $\sqrt{(SC_0 - Mean)^2} + \sqrt{(SC_1 - Mean)^2} + \sqrt{(SC_2 - Mean)^2} + \sqrt{(SC_3 - Mean)^2}$ (*Mean* is the mean value of SC_0 to SC_3).

图3　基于形态学MRI的测量参数对sym-SCA3、pre-SCA3及HCs两两鉴别的ROC曲线

Fig. 3　ROC curves of morphological MRI metrics for pair-wise identification among sym-SCA3、pre-SCA3 and HCs

参考文献

[1] Borbolla-Jiménez FV, Del Prado-Audelo ML, Cisneros B, et al. New Perspectives of Gene Therapy on Polyglutamine Spinocerebellar Ataxias: From Molecular Targets to Novel Nanovectors [J]. Pharmaceutics, 2021, 13(7).

[2] Klockgether T, Mariotti C, Paulson HL. Spinocerebellar ataxia[J]. Nat Rev Dis Primers, 2019, 5(1): 24.

[3] Schmitz-Hübsch T, Du Montcel ST, Baliko L, et al. Scale for the assessment and rating of ataxia: development of a new clinical scale[J]. Neurology, 2006, 66(11): 1717-1720.

[4] Wan N, Chen Z, Wan L, et al. MR Imaging of SCA3/MJD[J]. Front Neurosci, 2020, 14: 749.

[5] Maas RP, Van Gaalen J, Klockgether T, et al. The preclinical stage of spinocerebellar ataxias[J]. Neurology, 2015, 85(1): 96-103.

[6] Rezende TJR, De Paiva JLR, Martinez ARM, et al. Structural signature of SCA3: from presymptomatic to late disease stages[J]. Ann Neurol, 2018, 84(3): 401-408.

[7] Jacobi H, Reetz K, Du Montcel ST, et al. Biological and clinical characteristics of individuals at risk for spinocerebellar ataxia types 1, 2, 3, and 6 in the longitudinal RISCA study: analysis of baseline data[J]. Lancet Neurol, 2013, 12(7): 650-658.

[8] Wu X, Liao X, Zhan Y, et al. Microstructural Alterations in asymptomatic and symptomatic patients with spinocerebellar ataxia type 3: a tract-based spatial statistics study[J]. Front Neurol, 2017, 8: 714.

[9] Metwally MI, MaABasha, Abdelhamid GA, et al. Neuroanatomical MRI study: reference values for the measurements of brainstem, cerebellar vermis, and peduncles[J]. Br J Radiol, 2021, 94(1120): 20201353.

[10] Higashi M, Ozaki K, Hattori T, et al. A diagnostic decision tree for adult cerebellar ataxia based on pontine magnetic resonance imaging[J]. J Neurol Sci, 2018, 387: 187-195.

[11] Quattrone A, Nicoletti G, Messina D, et al. MR imaging index for differentiation of progressive supranuclear palsy from Parkinson disease and the Parkinson variant of multiple system atrophy [J]. Radiology, 2008, 246(1): 214-221.

[12] Reetz K, Rodríguez-Labrada R, Dogan I, et al. Brain atrophy measures in preclinical and manifest spinocerebellar ataxia type 2 [J]. Ann Clin Transl Neurol, 2018, 5(2): 128-137.

[13] Braga-Neto P, Godeiro-Junior C, Dutra LA, et al. Translation and validation into Brazilian version of the Scale of the Assessment and Rating of Ataxia (SARA) [J]. Arq Neuropsiquiatr, 2010, 68(2): 228-230.

[14] Sobana SA, Huda F, Hermawan R, et al. Brain MRI volumetry analysis in an indonesian family of SCA 3 patients: a case-based study [J]. Front Neurol, 2022, 13: 912592.

[15] Park YW, Joers JM, Guo B, et al. Assessment of Cerebral and cerebellar white matter microstructure in spinocerebellar ataxias 1, 2, 3, and 6 using diffusion MRI[J]. Front Neurol, 2020, 11: 411.

[16] Peng H, Liang X, Long Z, et al. Gene-related cerebellar neurodegeneration in SCA3/MJD: a case-controlled imaging-genetic study[J]. Front Neurol, 2019, 10: 1025.

[17] Fahl CN, Branco LM, Bergo FP, et al. Spinal cord damage in Machado-Joseph disease[J]. Cerebellum, 2015, 14(2): 128-132.

(编辑 余 菁)